A magnetic study of melt-spun $Nd_{10}Fe_{85}B_5$ ribbons

1998 J. Phys.: Condens. Matter 10 9081

(http://iopscience.iop.org/0953-8984/10/40/012)

J. Phys.: Condens. Matter **10** (1998) 9081–9092. Printed in the UK PII: S0953-8984(98)95020-2

A magnetic study of melt-spun $Nd_{10}Fe_{85}B_5$ ribbons

J Ding, Y Li and K Y Lee

Department of Materials Science, National University of Singapore, Singapore 119260

Received 11 June 1998, in final form 31 July 1998

Abstract. The structural and magnetic properties of $Nd_{10}Fe_{85}B_5$ ribbons produced by melt-spinning and subsequent annealing have been studied in this work. A mixture of $Nd_2Fe_{14}B$ and 13 vol.% of Fe was found in the ribbon melt-spun at 30 m s^{-1} and in samples subsequently annealed. ^{57}Fe-Mössbauer spectroscopy was used for phase analysis and for study of remanence enhancement. Remanence enhancement was found in ribbons after optimized treatment, after which ribbons consisted of 20–30 nm grains of $Nd_2Fe_{14}B$ and Fe phases. The remanence enhancement effect was attributed to both the soft and hard phases. Demagnetization processes have been studied. All samples exhibited single-phase behaviour, i.e. irreversible demagnetization processes of the hard and soft phases were synchronous even for samples consisting of sub-micron grains. No significant evidence of exchange-spring magnet behaviour was found for samples after optimum treatment. The exchange-spring magnet behaviour was observed in samples annealed at higher temperatures, at which the mean grain sizes were significantly larger than the domain wall thickness of Fe. The magnetic properties of $Nd_{10}Fe_{85}B_5$ ribbons in this work were associated with separation of soft Fe grains by $Nd_2Fe_{14}B$ grains because of a low fraction of Fe.

1. Introduction

Isotropic nanocrystalline magnetic materials with remanence enhancement are investigated in many research groups in the world, because these materials are interesting for both research and application [1–6]. The $Nd_2Fe_{14}B$/Fe nanocomposite is one of the most interesting candidates for economical permanent magnets [3, 4, 7]. As is well known, magnetic properties of nanocomposite materials are strongly dependent on microstructure and volume fraction of soft phases. Remanence enhancement is understood to be due to exchange coupling between magnetic spins in grain boundary areas of hard and soft magnetic phases. Unique magnetic properties, such as single magnetic phase behaviour, exchange-spring magnet behaviour and negative deviation of demagnetization remanence from the Wohlfarth relation [1, 4, 8], have been reported for nanocomposite magnetic materials.

In this work, we have studied magnetic properties of the $Nd_2Fe_{14}B$/Fe nanocomposite containing 13 vol.% of Fe in dependence on microstructure. The demagnetization processes will be reported in this paper. Magnetic properties of nanocomposite $Nd_{10}Fe_{85}B_5$ ribbons will be compared with those of other nanocomposites containing different amounts of soft phases. ^{57}Fe-Mössbauer spectroscopy has been used for characterization of remanence enhancement.

2. Experiment

The ingot of $Nd_{10}Fe_{85}B_5$ was prepared by arc-melting. Rapid solidification was carried out using a single copper wheel melt-spinner at a surface wheel speed of 30 m s^{-1} under

0953-8984/98/409081+12$19.50

pure argon atmosphere. As-spun ribbons were annealed at a temperature in the range of 300–1000 °C for 10 minutes under vacuum.

The as-spun ribbon and subsequently annealed ribbons were characterized using a Philips PW1710 x-ray diffractometer with Cu Kα radiation. Microstructure was examined using a JEOL JEM-100XII TEM transmission electron microscope. Ribbons were studied by ^{57}Fe-Mössbauer spectroscopy. Magnetic measurements were taken using an Oxford vibrating sample magnetometer (VSM) with a maximum applied field of 7162 kA m^{-1}. The magnetic field was applied parallel to the ribbon plane, to minimize the demagnetization field factor, so that the demagnetization field was negligibly small and was not considered.

3. Results and discussion

3.1. Microstructure and magnetic properties

No amorphous phase was present in the as-spun state by x-ray diffraction study. All ribbons (as-spun and subsequently annealed) consisted of a mixture of $Nd_2Fe_{14}B$ and α-Fe according to our x-ray diffraction measurements.

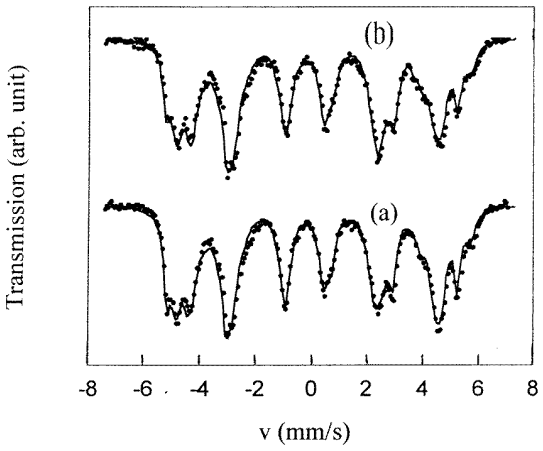

Figure 1. Mössbauer spectra of the as-spun sample in thermally demagnetized state (a) and in remanence state (b).

^{57}Fe-Mössbauer spectroscopy was used for phase analysis in this work. Figure 1 shows Mössbauer spectra of the as-spun sample. The Mössbauer spectra could be well fitted with the mixture of the two subspectra of $Nd_2Fe_{14}B$ and α-Fe respectively. All Mössbauer spectra of annealed samples were similar to that in figure 1(a) for the as-spun sample, showing that all samples had nearly the same phase constituents ($Nd_2Fe_{14}B$ and α-Fe). For all samples, 16–17% of Fe atoms were found in the α-Fe phase. This result agrees well with the calculated value of 17.6% of Fe atoms in the α-Fe phase for the composition of $Nd_{10}Fe_{85}B_5$ ($Nd_{10}Fe_{85}B_5 = 5Nd_2Fe_{14}B + 15Fe$).

From the composition of $Nd_{10}Fe_{85}B_5$, the calculated constituent is 87 wt% of $Nd_2Fe_{14}B$ and 13 wt% of Fe. Since the both phases have similar values of density, the volume fraction of Fe is 0.13, i.e. the sample consists of 13 vol.% of Fe and 87 vol.% of $Nd_2Fe_{14}B$. Taking the saturation magnetization of 170 A m^2 kg^{-1} for $Nd_2Fe_{14}B$ and 215 A m^2 kg^{-1} for Fe, the expected saturation magnetization of the $Nd_{10}Fe_{85}B_5$ ribbon is 176 A m^2 kg^{-1}.

Figure 2 shows TEM micrographs of the as-spun ribbon (a) and samples annealed at 850 °C (b) and 1000 °C (c) respectively. The as-spun ribbon and ribbons subsequently

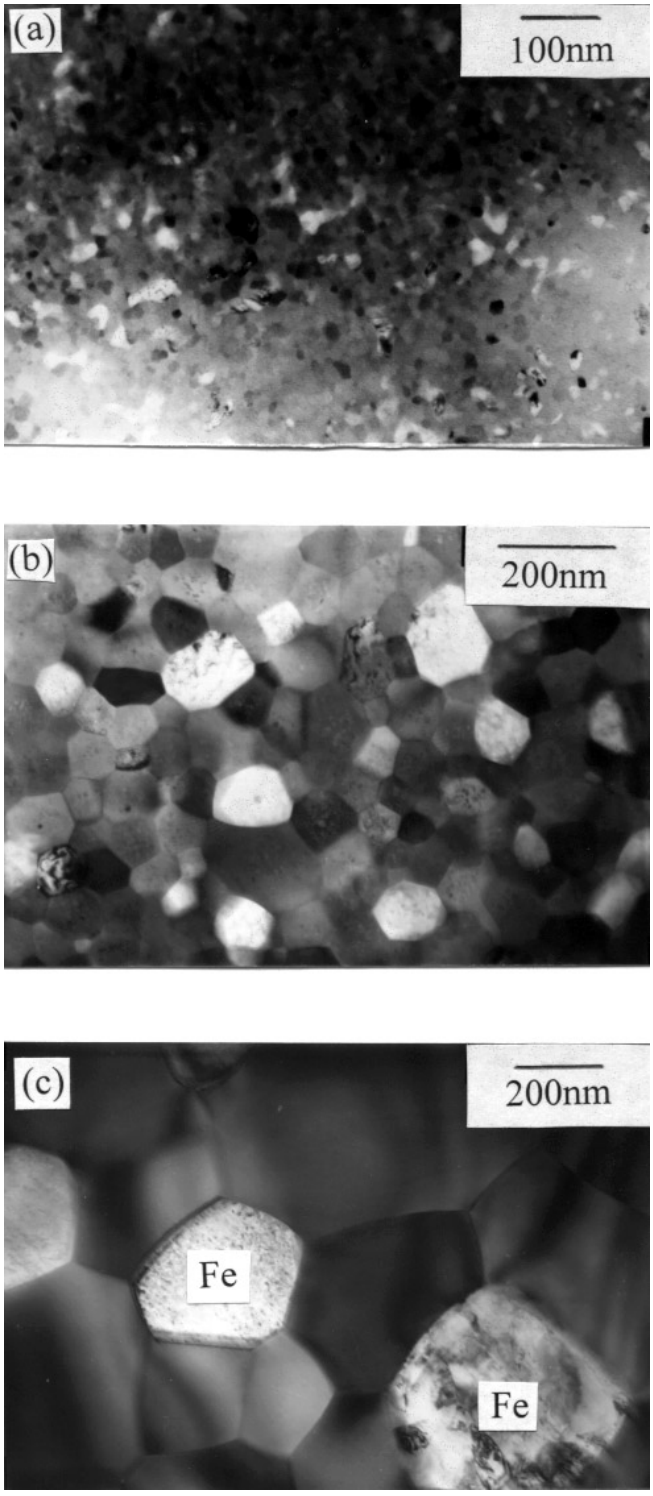

Figure 2. TEM micrographs of the as-spun sample (a) and ribbons subsequently annealed at 850 °C (b) and 1000 °C (c).

annealed at 300, 600 and 700 °C had a similar microstructure as shown in figure 2(a). There were two groups of grains under the transmission electron microscope, dark grains and bright grains (figure 2(a)). From electron diffraction rings, the dark grains should be $Nd_2Fe_{14}B$ grains which had a mean grain size of 20 nm, while the bright grains are probably α-Fe grains with a mean grain size of 30 nm.

The mean grain sizes of $Nd_2Fe_{14}B$ and Fe increased to 90 and 110 nm respectively after annealing at 850 °C, as shown in figure 2(b). After annealing at 1000 °C, α-Fe grains had a mean grain size of 210 nm. Large $Nd_2Fe_{14}B$ grains of up to 1000 nm were found, and the mean grain size was estimated to be 500 nm. Similar results of grain growth in dependence on annealing temperature have been reported previously [1, 2, 7].

Magnetic properties, such as remanence and coercivity, are plotted in figure 3 as a function of annealing temperature T_a. The coercivity for the as-spun ribbon was 560 kA m^{-1}. Coercivity remained unchanged after annealing at 300 and 600 °C, indicating that the samples annealed at lower temperatures had a similar microstructure as that of the as-spun sample. A slight decrease of coercivity was found for the sample annealed at 700 °C, from 560 to 500 kA m^{-1}. Annealing at higher temperatures led to drastic decrease of coercivity, 280 kA m^{-1} for the sample annealed at 850 °C and only 80 kA m^{-1} for the sample annealed at 1000 °C. Coercivity is strongly dependent on grain size. Increase of grain size normally leads to decrease of coercivity [1, 2, 7, 9]. The slight decrease of coercivity after annealing at 700 °C indicated initiation of grain growth. Low values of coercivity for samples annealed at 850 and 1000 °C respectively were due to presence of large grains (sub-micron grains in the sample annealed at 1000 °C). Similar results of decrease of coercivity due to grain growth have been reported previously [1, 2, 7, 9].

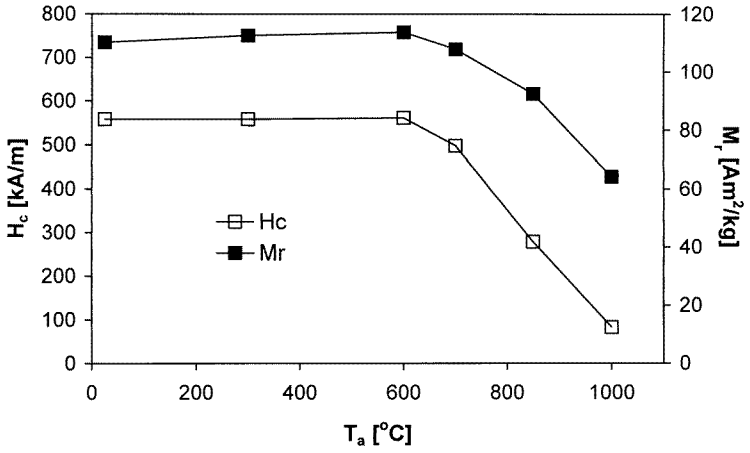

Figure 3. Coercivity H_c and remanence M_r as a function of annealing temperature T_a for $Nd_{10}Fe_{85}B_5$ ribbons.

Remanence M_r was 110 A m^2 kg^{-1} for the as-spun sample. It increased slightly to 114 A m^2 kg^{-1} after annealing at 600 °C. Taking the calculated saturation magnetization M_s of 176 A m^2 kg^{-1} for the composition of $Nd_{10}Fe_{85}B_5$, the remanence ratio (M_r/M_s) was 0.65 for $M_r = 114$ A m^2 kg^{-1}. Increase of grain size resulted in reduction of remanence and remanence ratio, 92 A m^2 kg^{-1} and $M_r/M_s = 0.52$ for the sample annealed at 850 °C, and 64 A m^2 kg^{-1} and 0.36 for the sample annealed at 1000 °C. This result confirms that

remanence enhancement (i.e. remanence exceeds half of saturation magnetization [1–6]) requires nanocrystalline structure. High remanence values can be obtained in nanocrystalline isotropic materials with grain sizes which are comparable with twice the domain wall thickness Δ ($2\Delta = 10$ nm for $Nd_2Fe_{14}B$ [1, 4, 5]).

Recently, Ding *et al* [10] and Ryan *et al* [11] have reported that Mössbauer spectroscopy can be used for study of remanence enhancement. As is well known, a six-line subspectrum (sextet) should have the line area ratio of 1:2:3 for isotropic materials in the thermally demagnetized state, where there is a random distribution of magnetic easy axes. In the remanence state, magnetizations of individual grains are parallel to their easy axes, if there is no remanence enhancement, i.e. $M_r = 0.5M_s$ [10, 11]. The line area ratio of 1:2:3 is also expected for isotropic materials in the remanence state. The Mössbauer spectrum of the thermally demagnetized as-spun $Nd_{10}Fe_{85}B_5$ sample is shown in figure 1(a). The line area ratio was close to 1:2:3 as expected for isotropic materials. Figure 1(b) is the Mössbauer spectrum of the $Nd_{10}Fe_{85}B_5$ sample in the remanence state. The magnetic field was applied parallel to the ribbon plane during the magnetization. The Mössbauer spectrum was taken when the γ-ray was perpendicular to the ribbon plane. Under this configuration of γ-ray and magnetization orientation, the line area ratio is expected to be 1:4:3, if all magnetic spins remain parallel to the applied magnetic field, i.e. perpendicular to the γ-ray [10, 11].

For the as-spun sample in the remanence state, the line area ratio was measured to be 1:2.9:3 and 1:3.1:3 for the $Nd_2Fe_{14}B$ phase and α-Fe respectively. The two line area ratios for the two phases ($Nd_2Fe_{14}B$ and α-Fe respectively) are between 1:2:3 for random distribution and 1:4:3 for perfect alignment, indicating remanence enhancement. This result shows that the remanence enhancement is attributed to both the hard and the soft phases, as the two phases had similar line area ratios.

Kneller and Hawig [1] have interpreted the remanence enhancement as mainly attributable to soft magnetic phases. Other theoretical works have shown that soft phases have a major contribution to remanence enhancement in nanocomposite materials [5, 12]. However, remanence enhancement has been observed in single-phase materials consisting of nanoscaled $Nd_2Fe_{14}B$ grains [4, 13, 14]. A few theoretical calculations have also shown that remanence enhancement can possibly be obtained in nanocrystalline single-phase materials [5, 15]. Therefore, the hard magnet phase has a contribution to remanence enhancement. In this work, both the hard and soft phases had a contribution to remanence enhancement according to our Mössbauer study. It is noteworthy that the mean grain size of Fe was 30 nm, which was bigger than that of $Nd_2Fe_{14}B$ (20 nm). Therefore, the soft phase (here α-Fe) may have a bigger contribution to remanence enhancement.

3.2. Demagnetization processes

As is well known, hysteresis loops of conventional magnetic materials consisting of soft and hard phases can show separated demagnetization processes of soft and hard phases [1, 2, 10]. This corresponds to two peaks of magnetic susceptibility in the demagnetization curves [1–4]. Nanocomposite magnets with remanence enhancement normally exhibit single-magnetic-phase behaviour [1–4], i.e. the irreversible demagnetization processes of hard and soft phases are synchronous. Increase of grain size in nanocomposite materials can result in decrease of remanence and coercivity. In the meantime, soft and hard magnetic phases are de-coupled, resulting in separation of demagnetization processes of hard and soft phases in hysteresis loops. It has been reported that many nanocomposite materials consisting of a mixture of soft and hard phases exhibit single-phase behaviour if grain sizes of hard and soft phases are comparable with twice the domain wall thickness, and two peaks of magnetic

susceptibility can be observed on the demagnetization curve after grain growth e.g., after annealing at higher temperatures [1–4, 6–8].

In this work, magnetic hysteresis and magnetic susceptibility were studied on $Nd_{10}Fe_{85}B_5$ ribbons in the as-spun state and after subsequent annealing. The hysteresis loop of the sample annealed at 600 °C (after optimized treatment) is shown in figure 4(a). The hysteresis loop is typical for nanocomposite materials with remanence enhancement, i.e. single-phase behaviour with relatively high values of remanence and coercivity. The as-spun sample and ribbons annealed at lower temperatures ($T_a \leqslant 700$ °C) had similar hysteresis loops to that shown in figure 4(a). The sample annealed at 850 °C had much lower values of coercivity and remanence because of grain growth. However, the hysteresis loop also showed single-phase behaviour. The sample annealed at 1000 °C, at which grains were increased to sub-micron, also exhibited single-phase behaviour. No significant separation of demagnetization processes of hard and soft phases was evident in the demagnetization curve of the sample annealed at 1000 °C (figure 4(b)).

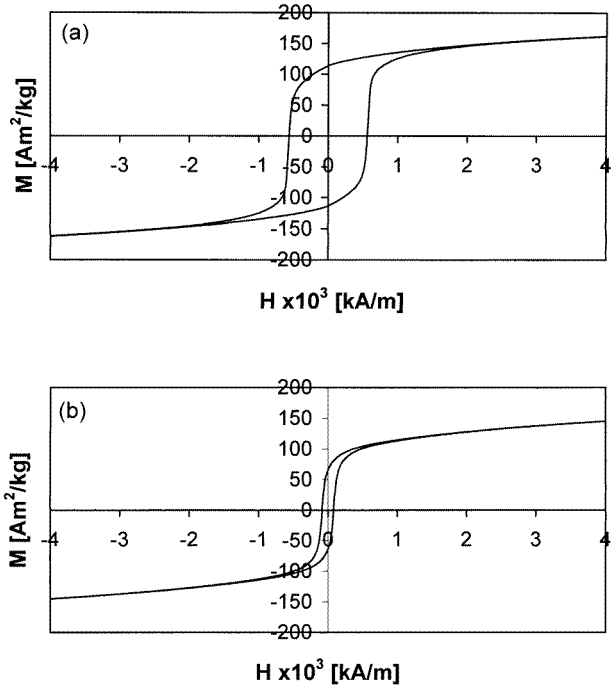

Figure 4. Hysteresis loops of the two ribbons annealed at 600 °C (a) and 1000 °C (b) respectively.

Figure 5 shows the plots of susceptibility curve on demagnetization for several samples annealed at 600, 850 and 1000 °C respectively. The as-spun sample and ribbons subsequently annealed at 300 and 600 °C respectively had shown their maximum of susceptibility close to the values of coercivity. Only a relative sharp peak was found on the demagnetization curve, showing single-magnetic-phase behaviour. The susceptibility curves of the samples annealed at 850 and 1000 °C respectively still had a single peak, which was close to the value of coercivity (figure 5). This behaviour confirms singe-phase behaviour for our samples as discussed above, i.e. no significant separation of demagnetization processes of $Nd_2Fe_{14}B$ and α-Fe was evident.

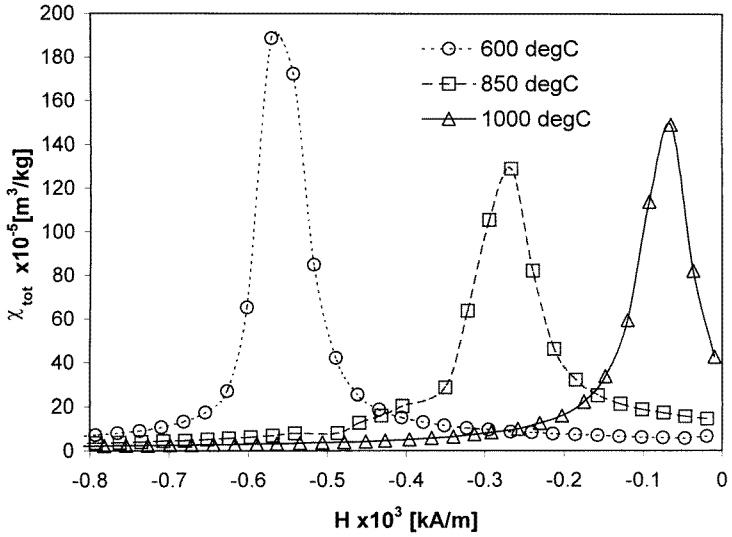

Figure 5. Total susceptibility χ_{tot} versus magnetic field H curve on demagnetization for several ribbons annealed at different temperatures for 10 min.

Another important feature of nanocomposite remanence enhanced magnets is exchange-spring magnet behaviour [1, 4, 10, 11, 16]. In this work, exchange-spring magnet behaviour was studied on $Nd_{10}Fe_{85}B_5$ ribbons. Demagnetization curves and recoil curves for the two samples annealed at 600 and 850 °C respectively are plotted in figure 6. Total, reversible and irreversible susceptibilities of both samples are shown in figure 7 as a function of magnetic field on their demagnetization curves. The recoil curves for the sample annealed at 600 °C were typical for conventional single-$Nd_2Fe_{14}B$-phase magnets [1, 4, 14]. From figure 7, it can be seen that total susceptibility is very close to irreversible susceptibility, and the reversible susceptibility is very small. These indicate that the exchange-spring magnet behaviour is not clearly evident for the sample annealed at 600 °C. For the sample annealed at 850 °C, exchange-spring magnet behaviour is observed as shown by recoil curves in figure 7(b). The total susceptibility at magnetic fields below coercivity was significantly above the irreversible susceptibility, resulting in detectable reversible susceptibility. It has been interpreted that reversible susceptibility at fields below coercivity is due to the reversible magnetization process of soft grains [1]. The rotation of soft grains toward the negative field occurs at magnetic fields which are below the coercivity of the sample. These soft grains can flip back to the positive direction after removal of magnetic field due to exchange coupling between grains of soft and hard phases [1, 4, 16].

The exchange-spring effect can be quantitatively described by susceptibility obtained from recoil curves, that samples showing exchange-spring magnet behaviour have high values of recoil susceptibility [4]. The $Nd_{10}Fe_{85}B_5$ sample annealed at 600 °C had a low value of recoil susceptibility. The reversible susceptibility measured on the recoil curves taken at fields around coercivity was 5–6 $\times$ 10^{-5} m^3 kg^{-1}. The sample annealed at 850 °C had a much higher recoil susceptibility (10–11 $\times$ 10^{-5} m^3 kg^{-1}). The recoil susceptibility increased to 24 $\times$ 10^{-5} m^3 kg^{-1} for the sample annealed at 1000 °C. This result shows clearly that the exchange-spring magnet behaviour became significant when the grain size of α-Fe increased above the single-domain particle size of Fe.

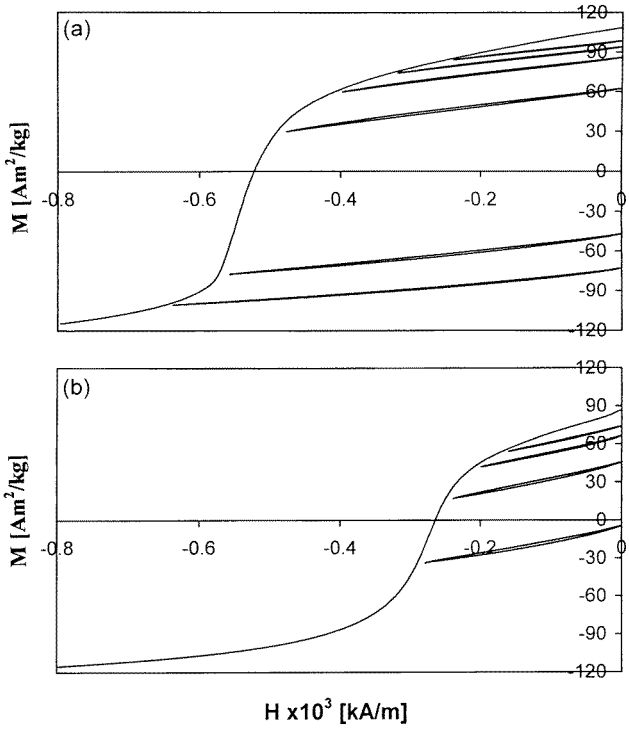

Figure 6. Demagnetization and recoil curves for ribbons annealed at 600 °C (a) and 850 °C (b) respectively.

Panagiotopoulos *et al* [4] have studied recoil curves of single $Nd_2Fe_{14}B$, $Nd_2Fe_{14}B$/Fe and $Nd_2Fe_{14}B/Fe_3B$. They have found that no significant exchange-spring magnet behaviour is evident for single-$Nd_2Fe_{14}B$-phase magnet with remanence enhancement and the recoil permeability is small. The recoil permeability was increased with increasing fraction of soft phases, indicating that exchange-spring magnet behaviour is mainly found for nanocomposite materials with a large amount of soft phases. We have also found similar results for single $Nd_2Fe_{14}B$ phase ribbons with remanence enhancement [14], that no exchange-spring magnet behaviour was evident.

As discussed above, 13 vol.% of Fe were present in $Nd_{10}Fe_{85}B_5$ ribbons. Fe grains should be surrounded by hard magnetic $Nd_2Fe_{14}B$ grains because of the relatively low fraction of Fe. The as-spun sample and ribbons annealed at a temperature below 600 °C consisted of a mixture of 20 nm $Nd_2Fe_{14}B$ and 30 nm α-Fe grains. The size of α-Fe though is bigger than twice the domain wall thickness of $Nd_2Fe_{14}B$ (10 nm), but still below the domain wall thickness of the α-Fe phase (50 nm). Because of strong coupling between isolated Fe grains and surrounding $Nd_2Fe_{14}B$ grains, Fe grains did not flip to the negative direction at low magnetic fields which were below coercivity. The flip of Fe grains was synchronous with the flip of surrounding $Nd_2Fe_{14}B$ also because of the strong exchange coupling. Therefore, the sample behaved as a single magnetic phase (figures 4 and 5) and no exchange-spring magnetic behaviour was evident (figures 6 and 7). The sample annealed at 850 °C consisted of $Nd_2Fe_{14}B$ grains of 90 nm and Fe grains of 110 nm. The grain size of Fe is then bigger than the domain wall thickness for α-Fe. Magnetic spins in some Fe

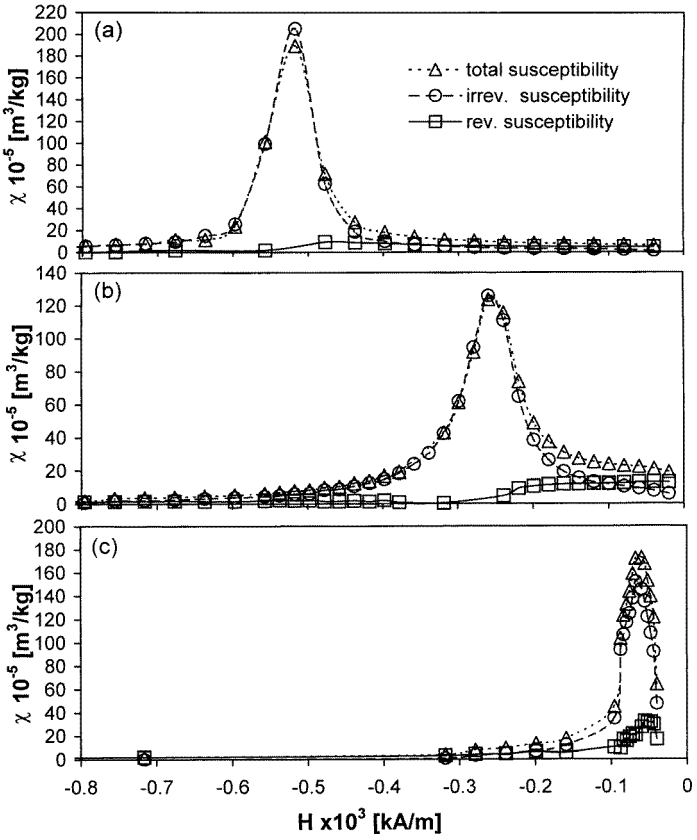

Figure 7. Total susceptibility χ_{tot}, irreversible susceptibility χ_{irr} and reversible χ_{rev} for $Nd_{10}Fe_{85}B_5$ ribbons annealed at 600 °C (a), 850 °C (b) and 1000 °C (c) respectively.

grains rotated toward the negative magnetic field at lower magnetic fields. This is probably the reason for the exchange-spring magnet behaviour observed in figure 6 and 7 for the sample annealed at 850 °C.

As reported previously, $Nd_2Fe_{14}B$/Fe with compositions close to $Nd_8Fe_{88}B_4$ or with lower Nd concentrations and $Nd_2Fe_{14}B/Fe_3B$ [1, 4, 10, 18] show exchange-spring magnet behaviour after optimized treatment, i.e. having a similar microstructure (grain sizes) of the as-spun $Nd_{10}Fe_{85}B_5$ ribbon in this work (figure 2(a)). In fact, $Nd_8Fe_{88}B_4$ corresponds to a phase constituent of 70 vol.% of $Nd_2Fe_{14}B$ and 30 vol.% of Fe [5, 7, 9]. $Nd_2Fe_{14}B/Fe_3B$ nanocomposites contain 60–70 vol.% of soft phases (Fe_3B and Fe) [1, 10, 17].

For $Nd_8Fe_{88}B_4$ consisting of 30 vol.% of Fe, Fe grains cannot be entirely separated by $Nd_2Fe_{14}B$ grains. Several Fe grains may be connected to form an Fe region. Such Fe regions may be much bigger than the grain size of Fe (20–30 nm). Some of these regions may have sizes which are close to or bigger than the domain wall thickness for Fe (50 nm). The higher the fraction of Fe the larger the mean size of Fe regions. It is probable that exchange-spring magnet behaviour requires the grain size or region size of soft phases of the order of domain wall thickness. This can be confirmed by the fact that $Nd_2Fe_{14}B/Fe_3B$ containing 60–70 vol.% of soft phases clearly shows exchange-spring magnet behaviour and reversible permeability increases with increasing Fe fraction for $Nd_2Fe_{14}B$/Fe composites

after optimum treatment. No significant exchange-spring magnet behaviour is observed in $Nd_{10}Fe_{85}B_5$ ribbons in this work, probably due to separation of soft Fe grains by hard $Nd_2Fe_{14}B$ grains, so that no large Fe regions could be formed in ribbons after optimized treatment.

The above discussion and conclusion may be applicable to the discussion of the result in figures 4 and 5. Clear separation of demagnetization processes has been observed in $Nd_2Fe_{14}B/Fe_3B$ nanocomposites after annealing at higher temperatures [1, 10], e.g. two steps of irreversible magnetization have been reported for $Nd_{4.5}B_{18.5}Fe_{77}$ ribbon annealed at 800 °C [10]. The microstructure (grain sizes) of the $Nd_2Fe_{14}B/Fe_3B$ nanocomposite annealed at 800 °C should not be significantly different to that of the $Nd_{10}Fe_{85}B_5$ ribbon annealed at 850 °C (figure 2(b)). The separation of demagnetization processes in $Nd_2Fe_{14}B/Fe_3B$ (consisting 60–70 vol.% of soft phases) may result from formation of soft regions, which can have a much larger size than the mean grain size of soft phases.

For $Nd_{10}Fe_{85}B_5$ ribbons in this work, the flip of isolated Fe grains was always accompanied by rotation of hard $Nd_2Fe_{14}B$ grains, as no separation of demagnetization processes was observed. This result shows that isolated Fe grains after flipping are nuclei which can cause demagnetization of neighbouring $Nd_2Fe_{14}B$ grains. The magnetic field required for flip of isolated Fe grains can be considered as the nucleation field for rotation of hard $Nd_2Fe_{14}B$ grains. On the other hand, a large fraction of soft phases (e.g. 60–70 vol.% for $Fe_2Nd_{14}B/Fe_3B$) may cause formation of large regions of soft phases. The presence of large soft regions may result in inhomogeneous microstructure. Large soft regions may lead to de-coupling of soft and hard grains, and therefore to separation of demagnetization processes of hard and soft phases.

It is also interesting to note that the appearance of two-magnetic-phase behaviour is strongly dependent on intrinsic properties of the hard phase, especially on the domain wall thickness [2, 9, 16, 19]. Miao *et al* [9] have reported that the substitution of Nd by Dy could result in separation of demagnetization processes in mechanically alloyed $(Nd,Dy)_2Fe_{14}B/Fe$, where no significant change of microstructure was evident. Separation of demagnetization processes have been observed in $(Nd \text{ or } Pr)_2Fe_{14}B/Fe$ nanocomposite, if the magnetic measurements were carried out at low temperature [19]. The two cases indicate that two-phase behaviour appears if the domain wall thickness of the hard phase is reduced, e.g. by substitution with Dy or by measurements at low temperature. Separation of demagnetization processes could be easily observed in $Sm_2Fe_{17}N_{2.7}/Fe$ nanocomposite even at lower Fe fractions, if the grain size exceeded the domain wall thickness of Fe [2]. That is probably because the $Sm_2Fe_{17}N_{2.7}$ phase has a much higher anisotropy field and therefore a smaller domain wall thickness than those for $Nd_2Fe_{14}B$. In fact, all nanocomposite magnetic materials with remanence enhancement have a similar microstructure (the mean grain size is 20–30 nm after optimum treatment [1, 2, 3, 7, 9]). It seems that hard magnetic phase with higher anisotropy field (or smaller domain wall thickness) requires smaller grain for optimum magnetic properties.

The Wohlfarth relationship [4, 8, 17] between remanent magnetization $M_r(H)$ and demagnetization remanence $M_d(H)$ has been widely used for study of interaction between magnetic particles and grains. The deviation of demagnetization remanence $M_d(H)$ from the demagnetization remanence calculated from the Wohlfarth model is expressed as below:

$$\Delta M_d = \frac{M_d(H) - (1 - 2M_r(H))}{M_{r,\max}}$$

where $M_{r,\max}$ is the maximum remanent magnetization measured after saturation in the positive direction.

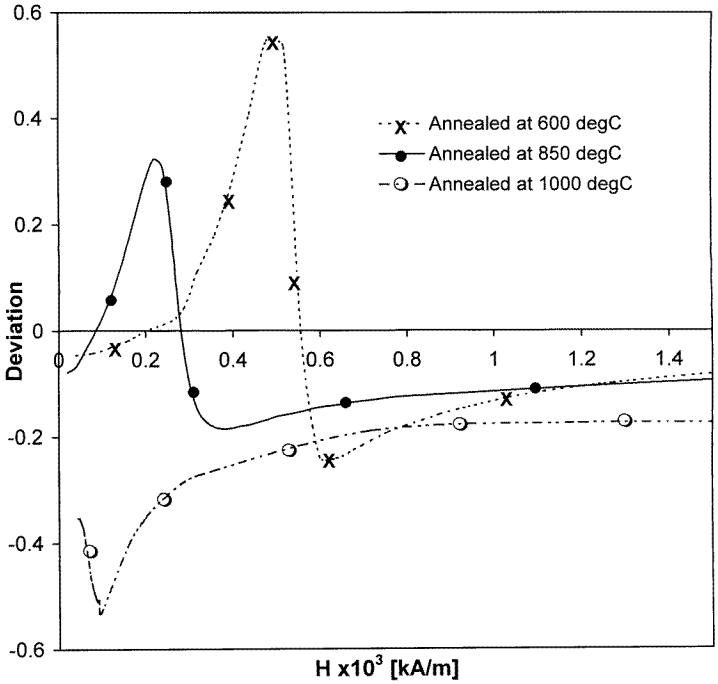

Figure 8. Deviation of demagnetization remanence ΔM_d from the Wohlfarth relationship for the ribbons annealed at 600, 850 and 1000 °C respectively.

Deviation ΔM_d from the Wohlfarth relation is plotted in figure 8 as a function of demagnetization field for three samples annealed at 600, 850 and 1000 °C respectively. The curve of the ribbon annealed at 600 °C is typical for nanocomposite materials with remanence enhancement. The large positive deviation at fields below coercivity has been interpreted as interaction between nanosized grains, and the negative deviation at fields above coercivity is probably due to magnetostatic interaction between soft and hard phases [4]. For the sample annealed at 850 °C, deviation (both positive and negative) was reduced, obviously due to reduction of inter-grain interaction because of increase of grain size. Large negative deviation was observed for the sample annealed at 1000 °C, indicating that the magnetostatic interaction was dominant because of large grain sizes for the $Nd_2Fe_{14}B$ and α-Fe phases in this sample.

4. Conclusion

An alloy of $Nd_{10}Fe_{85}B_5$ was melt-spun at a wheel speed of 30 m s^{-1}. The as-spun ribbon and subsequently annealed samples consisted of a mixture of $Nd_2Fe_{14}B$ and α-Fe. According to our Mössbauer spectroscopy study, the phase constituents were close to those for the starting composition of $Nd_{10}Fe_{85}B_5$, which corresponds to 13 vol.% of Fe and 87 vol.% of $Nd_2Fe_{14}B$.

As-spun ribbon and ribbons annealed at 300 and 600 °C had a similar microstructure, consisting of $Nd_2Fe_{14}B$ and Fe grains with mean grain sizes of 20 and 30 nm respectively. Annealing at higher temperatures resulted in increase of grain size. The mean grain sizes of $Nd_2Fe_{14}B$ and Fe were increased to 500 and 210 nm respectively after annealing at

1000 °C. Magnetic properties, such as remanence and coercivity, were strongly dependent on microstructure. The sample annealed at 600 °C possessed a coercivity of 560 kA m^{-1} and remanence of 114 A m^2 kg^{-1}, which was corresponding to 65% of the saturation magnetization. The ribbon annealed at 1000 °C had a low coercivity value of 80 kA m^{-1}, and the remanence was reduced to 64 A m^2 kg^{-1}.

The $Nd_2Fe_{14}B$/Fe nanocomposite in this work exhibited single-phase behaviour, i.e. demagnetization processes of the soft and hard phases were synchronous. This was probably due to the fact that Fe grains were separated by $Nd_2Fe_{14}B$ grains because of the relatively small fraction of α-Fe.

The sample annealed at 600 °C did not exhibit exchange-spring magnet behaviour, and the reversible susceptibility was very small. The sample annealed at 850 °C had larger grains and showed exchange-spring magnet behaviour. Since exchange-spring magnet behaviour was observed in $Nd_2Fe_{14}B$/Fe and $Nd_2Fe_{14}B/Fe_3B$ materials with larger fractions of soft phases, exchange-spring magnet behaviour is tentatively due to the presence of either large soft phase grains, which are comparable with the domain wall thickness of soft phase, or the formation of large regions of soft grains due to high soft phase fraction. Therefore, the exchange-spring magnet behaviour is probably the initialization of de-coupling of soft and hard phases. Further increase of grain size or soft region size results in separation of demagnetization processes of soft and hard phases. The exchange-spring magnet behaviour disappears if no coupling of soft and hard phases is present.

References

[1] Kneller E F and Hawig R 1991 *IEEE Trans. Magn.* **27** 3588
[2] Ding J, Liu Y, Street R and McCormick P G 1994 *J. Appl. Phys.* **75** 1032
[3] Manaf A, Buckley R A and Davies H A 1993 *J. Magn. Magn. Mater.* **128** 302
[4] Panagiotopoulos I, Withanawasam L and Hadjipanayis G C 1996 *J. Magn. Magn. Mater.* **152** 353
[5] Shrefl T, Fidler J and Kronmüller H K 1994 *Phys. Rev.* B **49** 6100
[6] Donnel K O, Kuhrt C and Coey J M D 1994 *J. Appl. Phys.* **76** 7068
[7] Miao W F, Ding J, McCormick P G and Street R 1996 *J. Alloys Compounds* **240** 200
[8] Patel V, El-Hilo M, O'Grady K and Chantrell R W 1993 *J. Phys. D: Appl. Phys.* **26** 1453
[9] Miao W F, Ding J, McCormick P G and Street R 1997 *J. Magn. Magn. Mater.* **175** 304
[10] Ding J, Street R and McCormick P G 1995 *J. Magn. Magn. Mater.* **140–144** 1071
[11] Ryan D H, Feutrill E H and Ding J 1997 *J. Appl. Phys.* **81** 4425
[12] Feutrill E H, McCormick P G and Street R 1994 *J. Appl. Phys.* **75** 5701
[13] McCallum R W, Kadin A M, Clemente G B and Keem J E 1987 *J. Appl. Phys.* **61** 3577
[14] Ding J, Li Y and Yong P T *J. Phys. D: Appl. Phys.* to be published
[15] Fukunaga H and Inoue M 1992 *Japan. J. Appl. Phys.* **31** 1347
[16] McCormick P G, Ding J, Feutrill E H and Street R 1996 *J. Magn. Magn. Mater.* **157–158** 7
[17] Müller K H, Eckert D, Handstein A and Nothnagel P 1992 *J. Magn. Magn. Mater.* **104–107** 1173
[18] Miao W F, McCormick P G and Street R 1997 *Solid State Commun.* **101** 687
[19] Withanawasam L, Murthy A S and Hadjipanayis G C 1995 *IEEE Trans. Magn.* **31** 3608